Axil, a Member of the Axin Family, Interacts with Both Glycogen Synthase Kinase 3β and β-Catenin and Inhibits Axis Formation of *Xenopus* Embryos

HIDEKI YAMAMOTO,[1] SHOSEI KISHIDA,[1] TAKAAKI UOCHI,[2] SATOSHI IKEDA,[1]
SHINYA KOYAMA,[1] MAKOTO ASASHIMA,[2] AND AKIRA KIKUCHI[1]*

*Department of Biochemistry, Hiroshima University School of Medicine, Minami-ku, Hiroshima 734-8551,[1] and
Department of Life Science (Biology), University of Tokyo, Meguro-ku, Tokyo 153-8902,[2] Japan*

Using a yeast two-hybrid method, we identified a novel protein which interacts with glycogen synthase kinase 3β (GSK-3β). This protein had 44% amino acid identity with Axin, a negative regulator of the Wnt signaling pathway. We designated this protein Axil for Axin like. Like Axin, Axil ventralized *Xenopus* embryos and inhibited Xwnt8-induced *Xenopus* axis duplication. Axil was phosphorylated by GSK-3β. Axil bound not only to GSK-3β but also to β-catenin, and the GSK-3β-binding site of Axil was distinct from the β-catenin-binding site. Furthermore, Axil enhanced GSK-3β-dependent phosphorylation of β-catenin. These results indicate that Axil negatively regulates the Wnt signaling pathway by mediating GSK-3β-dependent phosphorylation of β-catenin, thereby inhibiting axis formation.

Axin, which is a product of the mouse *Fused* locus, has been identified as a negative regulator of the Wnt signaling pathway (45). *Fused* is a mutation that causes dominant skeletal and neurological defects and recessive lethal embryonic defects including neuroectodermal abnormalities (36). Two spontaneous alleles of *Fused*, called *Kinky* (*Fu^Ki*) and *Knobbly* (*Fu^Kb*), and a transgenic insertional allele, *Fu^Tg1*, carry axis duplications and are lethal between 8 and 10 days postcoitus, suggesting that the *Fused* locus plays a role in the determination of the embryonic axis (9, 14, 33). The cDNA of this locus has been sequenced, and the *Fused* gene has been renamed Axin. Dorsal injection of wild-type Axin in *Xenopus* embryos blocks axis formation, and coinjection of Axin inhibits Wnt8-, dishevelled (Dsh)-, and kinase-negative glycogen synthase kinase 3β (GSK-3β)-induced axis duplication (45). These results suggest that Axin exerts its effects on axis formation by inhibiting the signal transduction in the Wnt signaling pathway. However, the molecular mechanism by which Axin regulates axis formation is not known.

Wnt and Wg signal many key developmental decisions, regulating anterior-posterior and dorsal-ventral patterns in both vertebrates and flies (22, 30, 31). In vertebrates, the Wnt signaling pathway consists of an intracellular cascade that includes frizzled, Dsh, GSK-3β, and β-catenin (5). The Wnts are a family of secreted polypeptides, whose receptors are believed to be members of the frizzled family (3). It has been suggested that Dsh acts downstream of frizzled (22, 30). GSK-3β is a constitutively active protein kinase and antagonizes downstream elements of the Wnt signaling pathway through changes in the β-catenin level (10). Wnt inactivates GSK-3β activity through Dsh, although by which mechanism is not known (6). In the presence of Wnt, there is a decrease in the phosphorylation of β-catenin and an increase in its stability, and β-catenin translocates to the nucleus (44). This translocation involves the association of β-catenin with the transcriptional enhancers of lymphocyte enhancer binding factor/T cell factor (LEF/TCF) family (2, 24). β-Catenin has a consensus sequence of a phosphorylation site for GSK-3β, and elimination of this possible phosphorylation site stabilizes β-catenin (22, 26, 44). It has been recently shown that the ubiquitination-proteasome pathway is involved in the degradation of β-catenin and that mutations in the GSK-3β consensus phosphorylation site of β-catenin prevent ubiquitination (1). It is well known that adenomatous polyposis coli gene product (APC) is required for the degradation of β-catenin, although the role of APC is not well understood (35). Furthermore, it has been shown that GSK-3β phosphorylates APC and that the phosphorylation enhances the binding of APC to β-catenin (37). Thus, it appears that GSK-3β is a key mediator in the Wnt signaling pathway to regulate β-catenin turnover and that the phosphorylation of β-catenin by GSK-3β is essential for this process. However, it is not clear how GSK-3β regulates the degradation of β-catenin since GSK-3β does not significantly phosphorylate β-catenin by the use of the mammalian purified proteins.

To obtain insights into the action of GSK-3β on the degradation of β-catenin and the specification of cell fate, we have tried to find a GSK-3β-interacting protein by using a yeast two-hybrid method. We isolated a protein which interacts with GSK-3β and found that this protein has 44% identity with Axin (45). We designated this protein Axil (Axin like). We show here that Axil inhibits Xwnt8-induced axis formation of *Xenopus* embryos like Axin. Further, we demonstrate that Axil makes a complex with both GSK-3β and β-catenin and that it promotes GSK-3β-dependent phosphorylation of β-catenin. These results suggest that Axil negatively regulates the Wnt signaling pathway by interacting with GSK-3β and β-catenin and by mediating the signal from GSK-3β to β-catenin, resulting in the regulation of axis formation.

MATERIALS AND METHODS

Materials and chemicals. Yeast strain L40, plasmid vectors for two-hybrid screening, and a pGAD10-derived rat brain cDNA library; pBSSK/GSK-3β; pBSSK/β-catenin; a λZAP rat brain cDNA library; pEF-BOS; pGEX-KG; a peptide substrate of GSK-3 (GSK peptide 1); the anti-hemagglutinin 1 (HA) antibody; and the anti-glutathione-*S*-transferase (anti-GST) and anti-maltose binding protein (anti-MBP) antibodies were kindly supplied by Y. Takai and K.

* Corresponding author. Mailing address: Department of Biochemistry, Hiroshima University School of Medicine, 1-2-3 Kasumi, Minami-ku, Hiroshima 734-8551, Japan. Phone: 81-82-257-5130. Fax: 81-82-257-5134. E-mail: akikuchi@mcai.med.hiroshima-u.ac.jp.

Tanaka (Osaka University, Suita, Japan), J. R. Woodgett (Ontario Cancer Institute, Toronto, Ontario, Canada), A. Nagafuchi and S. Tsukita (Kyoto University, Kyoto, Japan), Y. Hata (ERATO, Japan Science and Technology Corp., Kobe), S. Nagata (Osaka University) (23), F. Tamanoi (University of California, Los Angeles), C. W. Turck (University of California, San Francisco) (29), Q. Hu (Chiron Corp., Emeryville, Calif.), and M. Nakata (Sumitomo Electric Industries, Yokohama, Japan), respectively. The anti-Myc antibody was prepared from 9E10 cells. GST fused to GSK-3β (GST–GSK-3β) was purified from *Escherichia coli* as described previously (29). MBP fused to Axil (MBP-Axil), MBP fused to the Axil region including residues 265 to 483 [MBP-Axil(265-483)], MBP-Axil(265-412), MBP-Axil(412-483), GST–β-catenin, GST–β-catenin(1-423), and GST–β-catenin(423-781) were purified from *E. coli* according to the manufacturer's instructions. The anti-GSK-3β and anti-β-catenin antibodies were purchased from Transduction Laboratories (Lexington, Ky.). [α-^{32}P]dCTP and [γ-^{32}P]ATP were obtained from Amersham Inc. (Buckinghamshire, United Kingdom). Other materials were from commercial sources.

Plasmid construction. To construct pBTM116HA/GSK-3β, pBSSK/GSK-3β was digested with *Bcl*I and *Eco*RI and blunted with Klenow fragment. The 1.3-kb fragment was inserted into pBTM116HA, which was digested with *Bam*HI and blunted with Klenow fragment. To construct pCGN/GSK-3β^{K85M}, the 1.3-kb fragment encoding GSK-3β^{K85M} with *Xba*I and *Sma*I sites synthesized by PCR was inserted into the *Xba*I- and *Sma*I-cut pCGN. pCGN/GSK-3β and pGEX-2T/GSK-3β were constructed as described before (29). To construct pEF-BOS-Myc, the fragment encoding Myc epitope synthesized by PCR was inserted into pEF-BOS, which was digested with *Xba*I and blunted with Klenow fragment. To construct pBSSK/Axil, the 70-base fragment encoding Axil(1-23) with an *Sma*I site at the 5′ end was synthesized by PCR. This fragment was digested with *Sma*I and *Sac*II and inserted into the pBSKS containing the 3.2-kb fragment encoding Axil prepared from the library in pGAD10, which was digested with *Xba*I, blunted with Klenow fragment, and digested with *Sac*II. To construct pEF-BOS-Myc/Axil, pBSKS/Axil was digested with *Spe*I and *Xba*I and the 3.2-kb fragment encoding Axil was inserted into the *Xba*I-cut pEF-BOS-Myc. To construct pEF-BOS-Myc/Axil(1-670), pBSKS/Axil was digested with *Spe*I and *Sma*I and the 2.0-kb fragment encoding Axil(1-670) was inserted into the *Xba*I- and *Sma*I-cut pEF-BOS-Myc. To construct pBSKS/Axil(682-838), pGAD10/Axil(682-838) was digested with *Eco*RI and the 0.48-kb fragment encoding Axil(682-838) was inserted into the *Eco*RI-cut pBSKS. To construct pBJ-Myc/Axil(682-838), pBSKS/Axil(682-838) was digested with *Cla*I and *Xba*I and blunted with Klenow fragment. The 0.48-kb fragment encoding Axil(682-838) was inserted into pBJ-Myc, which was digested with *Bam*HI and blunted with Klenow fragment. To construct pEF-BOS/Myc-Axil(1-265), the fragment encoding Myc epitope-tagged Axil(1-265) with *Eco*RI and *Bam*HI sites synthesized by PCR was digested with *Eco*RI and *Bam*HI and blunted with Klenow fragment. The 0.85-kb fragment encoding Axil(1-265) was inserted into pEF-BOS, which was digested with *Xba*I and blunted with Klenow fragment. To construct pBSKS/Axil(265-483), the 0.66-kb fragment encoding Axil(265-483) with *Xba*I and *Bam*HI sites synthesized by PCR was inserted into the *Xba*I- and *Bam*HI-cut pBSKS. To construct pEF-BOS-Myc/Axil(265-483), pBSKS/Axil(265-483) was digested with *Xba*I and *Bam*HI and the 0.66-kb fragment encoding Axil(265-483) was inserted into the *Xba*I- and *Bam*HI-cut pEF-BOS-Myc. To construct pMAL-c2/Axil(265-483), pBSKS/Axil (265-483) was digested with *Xba*I and *Hin*dIII and the 0.66-kb fragment encoding Axil(265-483) was inserted into the *Xba*I- and *Hin*dIII-cut pMAL-c2. To construct pMAL-c2/Axil(265-412), the 0.45-kb fragment encoding Axil(265-412) with *Xba*I and *Hin*dIII sites was synthesized by PCR, digested with *Xba*I and *Hin*dIII, and inserted into the *Xba*I- and *Hin*dIII-cut pMAL-c2. To construct pMAL-c2/Axil(412-483), pMAL-c2/Axil(265-483) was digested with *Sac*I, the 0.45-kb fragment encoding Axil(265-412) was removed, and the remaining pMAL-c2 containing the fragment encoding Axil(412-483) was self-ligated. To construct pMAL-c2/Axil, pBSKS/Axil was digested with *Spe*I and *Xba*I and the 3.2-kb fragment encoding Axil was inserted into the *Xba*I-cut pMAL-c2. To construct pGEX-2T/β-catenin, pBSSK/β-catenin was digested with *Xho*I and blunted with Klenow fragment and the 2.7-kb fragment encoding β-catenin was inserted into the *Sma*I-cut pGEX-2T. To construct pGEX-2T/β-catenin(1-423), pBSSK/β-catenin was digested with *Bam*HI and *Eco*RI and the 1.3-kb fragment encoding β-catenin(1-423) was inserted into the *Bam*HI- and *Eco*RI-cut pGEX-2T. To construct pGEX-KG/β-catenin(423-781), pBSSK/β-catenin was digested with *Eco*RI and *Xho*I, and the 1.4-kb fragment encoding β-catenin(423-781) was inserted into the *Eco*RI- and *Xho*I-cut pGEX-KG.

Yeast two-hybrid screening and molecular cloning of Axil. A yeast strain L40 (*MAT*a *trp 1 leu2 his3 ade2 LYS2::lexA-HIS3 URA3::lexA-lacZ*) carrying pBTM116HA/GSK-3β was transformed with a rat brain cDNA library constructed in pGAD10 (12, 42). Approximately 3.7 × 10^6 transformants were screened for growth on SD plate medium lacking tryptophan, leucine, and histidine as evidenced by transactivation of a *lexA-HIS3* reporter gene and histidine prototrophy. His$^+$ colonies were scored for β-galactosidase activity. Plasmids harboring cDNAs were recovered from positive colonies, and the nucleotide sequences of plasmid DNAs which conferred the LacZ$^+$ phenotype on L40 containing pBTM116HA/GSK-3β were determined. To obtain a full-length cDNA of a GSK-3β-interacting protein, the clone isolated by the yeast two-hybrid method was labeled with random primers and [α-^{32}P]dCTP and used to screen a λZAP rat brain cDNA library. A number of positive clones were isolated, and all clones, collectively spanning 3.2 kb, were sequenced.

Xenopus **injections and analysis of phenotypes.** *Axil*, *Xwnt8*, and *Xglobin* cDNAs were individually subcloned into the *Bgl*II site of pSP64T (20). Sense mRNA was obtained by in vitro transcription of linearized templates by using the mCAP RNA capping kit (Stratagene, La Jolla, Calif.). Fertilized eggs were dejellied, and *Axil* mRNA (250 pg) was injected into dorsal or ventral blastomeres at the four-cell stage. *Xglobin* mRNA (250 pg) was injected into dorsal blastomeres at the four-cell stage. *Xwnt*8 mRNA (0.1 pg) was injected with or without *Axil* mRNA (250 pg) into ventral blastomeres at the four-cell stage. Injection was performed with 5% Ficoll in Steinberg's solution, and embryos were cultured for 2 days in Steinberg's solution. The phenotypes of the injected embryos were evaluated by the Dorso-Anterior Index (DAI) (15).

Interaction of GSK-3β and β-catenin with Axil. To determine whether Axil interacts with GSK-3β and β-catenin in intact cells, COS cells (10-cm-diameter dish) were transfected with pCGN-, pBJ-, and pEF-BOS-derived plasmids and lysed as described previously (16). Axil and its deletion mutants were tagged with Myc epitope at their N termini. GSK-3β and GSK-3β^{K85M} were tagged with HA epitope at their N termini. The lysates (500 to 1,000 μg of protein) were immunoprecipitated with the anti-Myc or anti-HA antibody, and then the precipitates were probed with the anti-Myc, anti-HA, anti-GSK-3β, and anti-β-catenin antibodies (11, 16, 28). To examine the interaction of β-catenin with Axil by using crude lysates in vitro, GST–β-catenin, GST–β-catenin(1-423), or GST–β-catenin(423-781) (50 pmol each) was incubated with the lysates (500 μg of protein) of COS cells expressing Myc-Axil for 2 h at 4°C. GST–β-catenin and its mutants were precipitated with glutathione Sepharose 4B, and the precipitates were probed with the anti-Myc antibody. To examine the interaction of GSK-3β and β-catenin with Axil by using the purified proteins in vitro, GST–GSK-3β or GST–β-catenin (8 pmol each) was incubated with MBP-Axil(265-483), MBP-Axil(265-412), or MBP-Axil(412-483) (2 pmol each) immobilized on amylose resin in 40 μl of reaction mixture (20 mM Tris-HCl [pH 7.5] and 1 mM dithiothreitol) for 2 h at 4°C. MBPs fused to proteins were precipitated by centrifugation, and the precipitates were probed with the anti-GSK-3β and anti-β-catenin antibodies.

Phosphorylation of Axil by GSK-3β. To examine the phosphorylation of full-length Axil by GSK-3β, the lysates (250 μg of protein) of COS cells expressing Myc-Axil were immunoprecipitated with the anti-Myc antibody. The precipitates were washed and incubated with or without GST–GSK-3β (100 ng of protein) in 30 μl of kinase reaction mixture (50 mM Tris-HCl [pH 7.5], 10 mM MgCl$_2$, 1 mM dithiothreitol, 50 μM [γ-^{32}P]ATP [500 to 2,000 cpm/pmol]) for 20 min at 30°C. When kinetics for the phosphorylation of Axil by GST–GSK-3β was examined, MBP-Axil(265-483) purified from *E. coli* was used as a substrate. The samples were subjected to sodium dodecyl sulfate-polyacrylamide gel electrophoresis (SDS-PAGE) followed by autoradiography. Where specified, the radioactivities of phosphorylated Axil were counted.

Phosphorylation of β-catenin by GSK-3β in the presence of Axil. GST–β-catenin or GST–β-catenin(1-423) (2 μg of protein each) was incubated with GST–GSK-3β (400 or 600 ng of protein) in the presence of several deletion mutants of MBP-Axil (200 ng of each protein) or MBP-Axil (160 ng of protein) in 30 μl of kinase reaction mixture for 30 min at 30°C. The samples were subjected to SDS-PAGE followed by autoradiography. When the amounts of phosphate incorporated into GST–β-catenin were determined, the radioactivities of phosphorylated GST–β-catenin were counted.

Other assays. Northern blot analysis was performed as described previously (21). Protein concentrations were determined with bovine serum albumin as a standard (4). When the effect of Axil on the GSK-3β activity was examined, GST–GSK-3β (400 ng of protein) was incubated with 50 μM GSK peptide 1 in the presence of MBP-Axil(265-483) or MBP-Axil in 30 μl of kinase reaction mixture for 10 min at 30°C. The reaction mixture was then spotted on phosphocellulose filters and washed with phosphoric acid (29).

Nucleotide sequence accession number. The GenBank accession number for rat *Axil* cDNA is AF017757.

RESULTS

Isolation of GSK-3β-interacting protein. To identify proteins that physically interact with GSK-3β, we conducted a rat brain cDNA library screening by the yeast two-hybrid method. We identified four partial cDNA clones that specifically interact with GSK-3β. Among these clones, two were found to encode a sequence of 94% identity with the sequence of mouse Axin, and we designated this protein rAxin for rat Axin (13). Since another clone had a high percentage of GC base pairs (62%), we did not characterize it further. The remaining clone encoded a novel protein. Therefore, we will focus on this clone in this report.

A full-length cDNA of this GSK-3β-interacting protein was isolated from a rat brain cDNA library. This clone spanned a distance of 3.2 kb and contained an uninterrupted open reading frame of 2,514 bp, encoding a predicted protein of 838

A

```
Axil    1:MSS---AVLVTLLF-DPSSSFREDAPRPPVPGEEGE-----TPPCQPS--  39
rAxin   1:MQSPKMNVQEQGFPLDLGASFTEDAPRPPVPGEEGELVSTDSRPVNHSFC  50

Axil   40:VGKVQSTKPMPVSSNARRNEDGLG-EPEGRASPDSPLTRWTKSLHSLIGD  88
rAxin  51:SGKGTSIKSETSTATPRRSDLDLGYEPEGSASPTPPYLWTAESLHSLIDD 100

Axil   89:QDGAYLFRTFLEREKCVDTLDFWFACNGFRQMNLKD---TKTLRVAKAIY 135
rAxin 101:QDGISLFRTFLKQEGCADLLDFWFACSGFRKLEPCDSNEEKRLKLARAIY 150

Axil  136:KRYI-ENNSVVSKQLKPATKTYIRDGIKKQQIGSVMFDQAQTEIQAVMEE 184
rAxin 151:RKYILDSNGIVSRQTKPATKSFIKDCVMKQQIDPAMFDQAQTEIQSTMEE 200

Axil  185:NAYQVFLTSDIYLEYVRSGGENTAYMS--NGGLGSLKVLCGYLPTLNEEE 232
rAxin 201:NTYPSFLKSDIYLEYTRTGESEPKVCSDQSSCSCTGKGMSGYLPTLNEDE 250

Axil  233:EWTC---AD-LKCKLSPTVVGLSSKTLRATASVR---STETAE-NGFRSF 274
rAxin 251:EWKCDQDADEDDGRDSVPPSRLTQKLLLETAAPRAPSSRRYNEGRELRYG 299

Axil  275:KRSEPVNPYHVGSGYVFAPATSANDSE---LSSSDALTDDSMSMTDSSVDG 321
rAxin 301:SWREPVNPYYVNSGYALAPATSANDSEQQSLSSDA---DTLSLTDSSVDG 347

Axil  322:IPPYRMGSKKQLQREMHRSVKANGQVSLPHFPRTHRLPKEMTPVEPAAFA 371
rAxin 348:IPPYR--IRKQHRREMQESVQVNGRVPLPHIPRTYRMPKE-IRVEPQKFA 394

Axil  372:AELISRLEKLKLELESRHSLEERLQQIREDEEKEGSE-----QALSSRDG 416
rAxin 395:EELIHRLEAVQRTREAEEKLEERLKRVRMEEEGEDGEMPSGPMASHKLPS 444

Axil  417:APVQH-----PLALLPSG---SYEEDPQTILDDHLSRVLKTPGCQSPGVG 458
rAxin 445:VPAWHHFPPRYVDMGCSGLRDAHEENPESILDEHVQRVMRTPGCQSPC-- 492

Axil  459:RYSPRSRSPDHHHHHTQQCHALLPTCGKLPPEAACPLLGGK-SFLTKQTT 507
rAxin 493:---PGHRSPD---SGTVAKTAVL-GCTASGHGKHAPKLCLKLDSAGLHHH 535

Axil  508:KHVHHHYIHHHAVPKTKEEIEAEATQRVRCLCPGC--TDYYCYSKCKSHS 555
rAxin 536:RHVHHHVHHNSARP--KEQMEAEAARRVQSSFSWCPETHGHAKPRSYSES 583

Axil  556:KPPEELPCEQFCCSRGGTLPKRNTKCTEPCLALPAREGGMSSAAGAPCLP 605
rAxin 584:TGTNPSAGDLAFCGKASAPSKRNTKKAESCKNASAEVPSTTEDAEKNC-- 631

Axil  606:GEEGDRSCDVWQWMLESERQSKSKPHSTQSIRKSYPLESARAPPGERVSR 655
rAxin 632:----KIMQWIIEGEKEISRHRK-AGHGSSGMRKQQAHESSRPLSIERPGA 676

Axil  656:HHLLGASGHPRSAARAHPFTQDPAMPPLTPPNTLAQLEEACRRLAEVSKP 705
rAxin 677:VHPWVSAQLRNSVQPSHLFIQDPTMPPNPAPNPLTQLEEARRRLEE---E 723

Axil  706:QKQRCCVASCQQRDRNHPATGQAGPTSFSNPSLASEDHKEPKRLASVHALQ 755
rAxin 724:EKRANKLPSKQR---TKSQRKACGGS--------------------APP 749

Axil  756:ASELIVTYYFFCGEEIPYRRMLKAQSLTLGHFKEQLSKKGNYRYYFKKASD 805
rAxin 750:CDSIVVAYYFCGEPIPYRTLVRGRAVTLGQFKELITKKGSYRYYFKKVSD 799

Axil  806:EFACGAVFEEIWDDETVLPMYEGRILGKVERID 838
rAxin 800:EFDCGVVFEEVREDEAILPVFEEKIIGKVEKVD 832
```
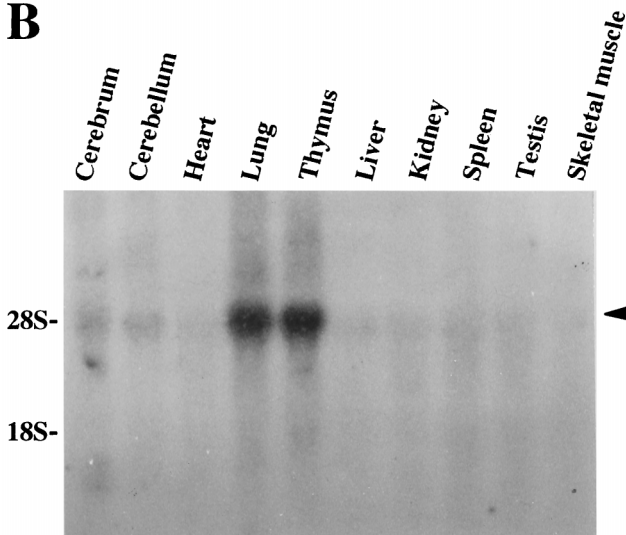
B

FIG. 1. Structure of Axil. (A) Amino acid sequence of Axil. Identical residues in Axil and rAxin are denoted by a black background. The RGS homologous and Dsh homologous domains are boxed. (B) Northern blot analysis of Axil. Total RNAs (20 μg/lane) of various rat tissues were probed with cDNA encoding Axil(1-148). The positions of 28S and 18S ribosomal RNAs are indicated. The arrowhead indicates the positions of *Axil* mRNA. The results shown are representative of two independent experiments.

amino acids with a calculated M_r of 92,946 (Fig. 1A). The first ATG was preceded by stop codons in all three reading frames and the 5′-noncoding region had a high percentage of GC base pairs (86%). The neighboring sequence of the first ATG was consistent with the translation initiation start proposed by Kozak (19). This protein was found to have 44% amino acid identity with rAxin, so we designated this GSK-3β-interacting protein Axil (Axin like) (Fig. 1A). Like Axin, Axil had two domains which are homologous to regulators of G protein signaling (RGS) and Dsh. The N-terminal region of Axil, residues 77 to 200, had 29% amino acid identity with residues 58 to 178 of RGS4, which has been identified as a GTPase-activating protein (GAP) for heterotrimeric GTP-binding protein (G protein) (8). The C-terminal region, residues 763 to 826, had 35% amino acid identity with residues 8 to 73 of the mouse Dsh homolog, DVL-1 (41). A single band of 4.9-kb *Axil* mRNA was detected in various rat tissues and was highly expressed in lung and thymus (Fig. 1B).

Effect of Axil on axis formation of *Xenopus* embryos. It has been demonstrated that Axin regulates axis formation of *Xenopus* embryos (45). Therefore, we examined the effect of Axil on embryonic axis formation. When *Axil* mRNA was injected into the dorsal blastomeres at the four-cell stage, these embryos showed various ventralized phenotypes such as loss of head and microcephaly (Fig. 2A and B; Table 1). However, embryos injected ventrally with *Axil* mRNA developed normally (Fig. 2C; Table 1). Control injection of *Xglobin* mRNA had no effect (Fig. 2D; Table 1). Xwnt8 has been shown to induce a secondary dorsal axis when injected into the ventral side of the embryos (40). Coinjection of *Axil* mRNA blocked the *Xwnt8* mRNA-induced secondary axis formation (Table 2). These results suggest that Axil inhibits either normal or secondary dorsal axis formation in *Xenopus* embryos by interfering with the Wnt signaling pathway. Therefore, it appears that Axil has the same activity to regulate axis formation as Axin.

Interaction of Axil with GSK-3β. Previously, we found that GSK-3β is expressed in COS cells (29). To examine whether Axil interacts with endogenous GSK-3β in intact cells, we expressed Myc-Axil in COS cells (Fig. 3A). When the lysates expressing Myc-Axil were immunoprecipitated with the anti-Myc antibody, endogenous GSK-3β was detected in the Myc-Axil immune complex (Fig. 3A). Neither Myc-Axil nor GSK-3β was immunoprecipitated from the lysates expressing Myc-Axil with nonimmune immunoglobulin (data not shown). GSK-3β^{K85M}, in which the ATP binding site is mutated, is known to be a catalytically inactive mutant. Cotransfection of Myc-Axil with wild-type HA–GSK-3β or HA–GSK-3β^{K85M} did not alter the level of expression of transfected Myc-Axil as assessed by immunoblot analysis (Fig. 3B). When these lysates were immunoprecipitated with the anti-HA antibody, Myc-Axil was coprecipitated with wild-type HA–GSK-3β but not with HA–GSK-3β^{K85M} (Fig. 3B). These results demonstrate that Axil makes a complex with GSK-3β in intact cells and that the kinase activity of GSK-3β is necessary for its complex formation with Axil.

Phosphorylation of Axil by GSK-3β. To determine whether Axil is a substrate for GSK-3β, Myc-Axil immunoprecipitated from COS cell lysates was incubated with or without GST–GSK-3β. Myc-Axil was phosphorylated without GST–GSK-3β, and this phosphorylation was enhanced by GST–GSK-3β (Fig.
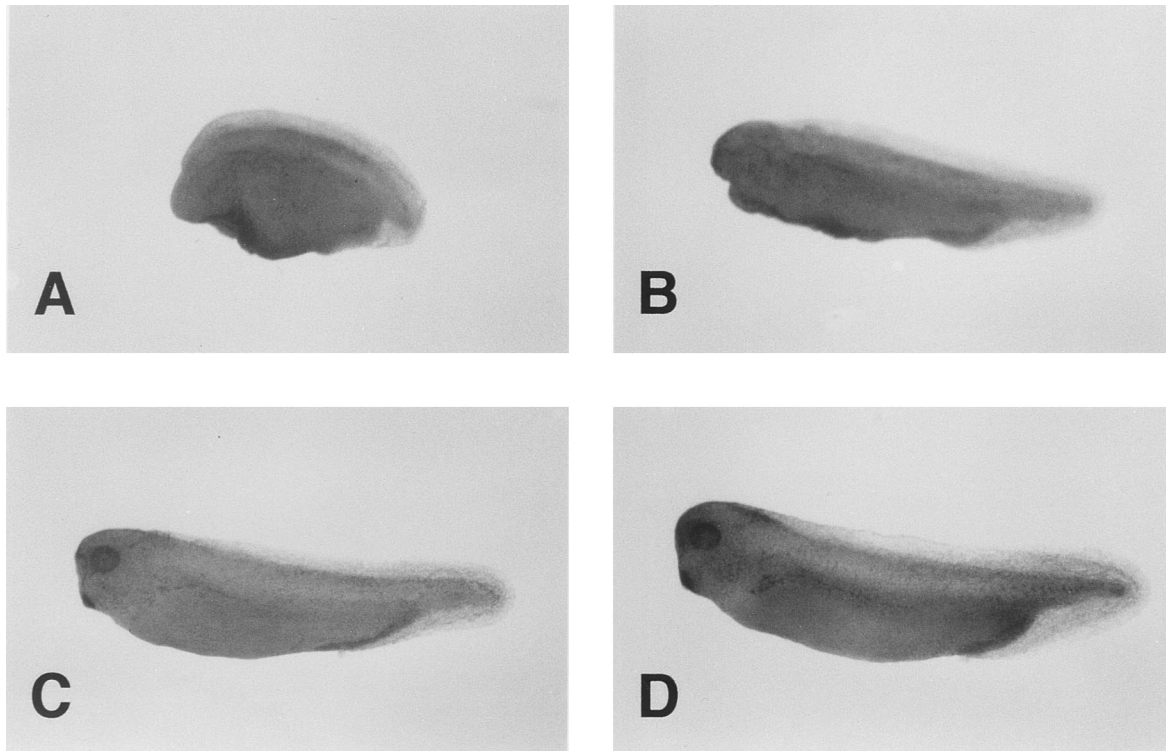
FIG. 2. Effect of Axil on axis formation of *Xenopus* embryos. (A and B) Dorsal injection of *Axil* mRNA. The embryo has no head region (DAI = 1) (A) or has microcephaly (DAI = 3) (B). (C) Ventral injection of *Axil* mRNA. (D) Control injection of *Xglobin* mRNA. Embryos were evaluated at the tail bud stage, and examples are shown.

4A). GST–GSK-3β phosphorylated Myc-Axil in time- and dose-dependent manners (Fig. 4B and C). In Fig. 3, we showed that endogenous GSK-3β is coprecipitated with Myc-Axil. Therefore, the phosphorylation of Myc-Axil without GST–GSK-3β might be due to the associated endogenous GSK-3β. However, we cannot rule out the possibility that GSK-3β phosphorylates and activates other protein kinases which interact with and phosphorylate Myc-Axil. Alternatively, other protein kinases which interact with Myc-Axil might phosphorylate it independently of GSK-3β.

Interaction of Axil with β-catenin. It has been demonstrated that Axin negatively regulates the Wnt signaling pathway downstream of GSK-3β and upstream of β-catenin (45). As shown in Fig. 2, we have found that Axil also inhibits the Wnt signaling pathway to induce axis duplication like Axin. Therefore, we next examined the relationship between Axil and β-catenin. When the lysates expressing Myc-Axil were immunoprecipitated with the anti-Myc antibody, endogenous β-catenin was coprecipitated with Myc-Axil (Fig. 5A). Neither Myc-Axil

nor β-catenin was immunoprecipitated from the lysates expressing Myc-Axil with nonimmune immunoglobulin (data not shown). To determine the region of β-catenin which interacts with Axil, GST–N-terminal β-catenin(1-423) and GST–C-terminal β-catenin(423-781) were purified from *E. coli*. Myc-Axil was coprecipitated with GST–N-terminal β-catenin but not with GST–C-terminal β-catenin (Fig. 5B). These results indicate that Axil makes a complex with the N-terminal region of β-catenin in intact cells.

Complex formation of GSK-3β, Axil, and β-catenin. From the results of Fig. 3 and 5, we found that Axil makes a complex with both GSK-3β and β-catenin. Therefore, we examined whether these three proteins make a ternary complex. When Myc-Axil and HA–GSK-3β were coexpressed in COS cells and HA–GSK-3β was immunoprecipitated with the anti-HA antibody, both Myc-Axil and endogenous β-catenin were detected in the HA–GSK-3β immune complex (Fig. 6A). These results suggest that GSK-3β, Axil, and β-catenin make a ternary complex in intact cells, although caution is necessary in interpreting

TABLE 1. Frequency and extent of ventralization by dorsal injection of *Axil* mRNA[a]

mRNA and region	No. (%) of embryos with phenotype			No. (%) of dead	No. of specimens	% Ventralized embryos	Avg DAI
	Normal	Microcephaly	Headless				
Axil							
Dorsal blastomere	4 (9.3)	11 (25.6)	21 (48.8)	7 (16.3)	43	74.4	1.9
Ventral blastomere	27 (90)	0	2 (6.7)	1 (3.3)	30	6.7	4.7
Xglobin: dorsal blastomere	48 (90.6)	4 (7.5)	0	1 (1.9)	53	7.5	4.7

[a] All mRNAs were injected into the subequatorial region of two dorsal or ventral blastomeres of four-cell embryos. The Dorso-Anterior Index (DAI) is a measure of axial development, where 5 is normal and 0 is completely ventralized (15).

TABLE 2. Frequency of axis duplication by ventral
injection of *Axil* and *Xwnt8* mRNA[a]

mRNA and region	No. of embryos with phenotype		No. of dead	No. of specimens	% of specimens with axis duplication
	Normal	Axis duplication			
Xwnt8: ventral blastomere	18	30	1	49	61.2
Axil + *Xwnt8*: ventral blastomere	36	11	1	48	22.9

[a] All mRNAs were injected into the subequatorial region of two ventral blastomeres of four-cell embryos.

these results until a gel filtration experiment shows that all three components are present in a large complex. To examine which region of Axil interacts with GSK-3β and β-catenin, several deletion mutants of Myc-Axil were expressed in COS cells (Fig. 6B). When these Myc-Axil mutants were immunoprecipitated with the anti-Myc antibody, Myc-Axil(1-670) and Myc-Axil(265-483) made a complex with both GSK-3β and β-catenin like Myc-Axil(full length) did (Fig. 6C). Neither GSK-3β nor β-catenin was coprecipitated with Myc-Axil(682-838) (Fig. 6C). Although GSK-3β was not detected in the Myc-Axil (1-265) immune complex, β-catenin was faintly coprecipitated (Fig. 6C). These results demonstrate that the region containing residues 265 to 483 of Axil is responsible for making a complex with both GSK-3β and β-catenin. To characterize this region, MBP-Axil(265-483), MBP-Axil(265-412), and MBP-Axil(412-483) were purified from *E. coli*. MBP-Axil(265-483) bound to both GST–GSK-3β and GST–β-catenin. Furthermore, MBP-Axil(265-412) and MBP-Axil(412-483) bound to GST–GSK-3β and GST–β-catenin, respectively (Fig. 6D). These results clearly show that GSK-3β and β-catenin directly interact with different sites on Axil. Sequence S/TXXXS/T is known to be a consensus sequence for a GSK-3β phosphorylation site (34). In residues 265 to 483 of Axil, there are four possible phosphorylation sites for GSK-3β: SFKRS[277], SANDSELSSDALT[308], SMSMT[315], and SMTDS[317] (S and T mean the possible phosphorylation residues by GSK-3β). Indeed, MBP-Axil(265-483)

was directly phosphorylated by GST–GSK-3β (Fig. 6E). GST–GSK-3β phosphorylated MBP-Axil(265-483) in a time-dependent manner, and 1.8 mol of phosphate was maximally incorporated into 1 mol of MBP-Axil(265-483) (Fig. 7A). The K_m and V_{max} values for the phosphorylation of Axil(265-483) by GSK-3β were calculated to be 6.4 nM and 580 pmol/min/mg, respectively (Fig. 7B). Since the K_m value of Axil(265-483) is much lower than those of other known substrates such as inhibitor-2, myelin basic protein, and κ-casein (43), Axil could be a good substrate for GSK-3β, although the K_m value of full-length Axil for GSK-3β remains to be clarified.

Phosphorylation of β-catenin by GSK-3β in the presence of Axil. It has been shown that β-catenin has a consensus sequence of the phosphorylation site for GSK-3β and that β-catenin mutants lacking this site are more stable than the wild type (26, 44). Therefore, it is thought that the phosphorylation of β-catenin by GSK-3β regulates the stability of β-catenin. Compared with the phosphorylation of GST–β-catenin by GST–GSK-3β in the absence of MBP-Axil(265-483), MBP-Axil(265-483) increased GST–GSK-3β-dependent phosphorylation of GST–β-catenin fivefold (Fig. 8A). Approximately 0.02 and 0.1 mol of phosphates were incorporated into 1 mol of GST–β-catenin in the absence and presence of MBP-Axil(265-483), respectively. However, neither MBP-Axil(265-412) nor MBP-Axil(412-483) affected the phosphorylation (Fig. 8A). These results demonstrate that Axil promotes GSK-3β-dependent phosphorylation of β-catenin and that the enhancement of GSK-3β-dependent phosphorylation of β-catenin by Axil requires both the GSK-3β- and β-catenin-binding sites of Axil. We also examined the effect of full-length Axil on GSK-3β-dependent phosphorylation of β-catenin. It was difficult to purify MBP-Axil from *E. coli*, and degradation products were observed on SDS-PAGE (data not shown). Since the M_rs of GST–β-catenin and MBP-Axil were similar, GST–N-terminal β-catenin [GST–β-catenin(1-423)], which contains the phosphorylation site for GSK-3β, was used in this experiment. As expected, MBP-Axil enhanced the phosphorylation of GST–N-terminal β-catenin by GST–GSK-3β (Fig. 8B). Since neither MBP-Axil(265-483) nor MBP-Axil affected the GST–GSK-3β activity to phosphorylate GSK peptide 1 under the condition that Axil promoted
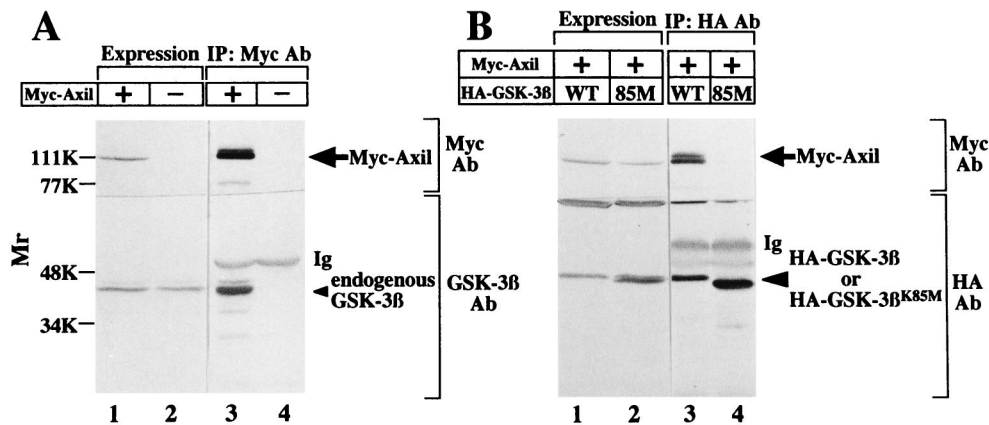

FIG. 3. Interaction of Axil with GSK-3β. (A) Interaction of Axil with endogenous GSK-3β in COS cells. The lysates (20 μg of protein) of COS cells expressing Myc-Axil were probed with the anti-Myc and anti-GSK-3β antibodies (lane 1). The same lysates (500 μg of protein) were immunoprecipitated with the anti-Myc antibody, and the immunoprecipitates were probed with the anti-Myc and anti-GSK-3β antibodies (lane 3). The lysates of COS cells transfected with empty vectors were used as controls (lanes 2 and 4). (B) Requirement of kinase activity of GSK-3β for its interaction with Axil. Myc-Axil was coexpressed with wild-type HA–GSK-3β (lanes 1 and 3) or HA–GSK-3β[K85M] (lanes 2 and 4) in COS cells, and the lysates were probed with the anti-Myc and anti-HA antibodies (lanes 1 and 2) or immunoprecipitated with the anti-HA antibody. The immunoprecipitates were then probed with the anti-Myc and anti-HA antibodies (lanes 3 and 4). IP, immunoprecipitation; Ab, antibody; Ig, immunoglobulin; WT, wild type HA–GSK-3β; 85M, HA–GSK-3β[K85M]. The arrows, small arrowhead, and large arrowhead indicate the positions of Myc-Axil, endogenous GSK-3β, and HA–GSK-3β or HA–GSK-3β[K85M], respectively. The results shown are representative of three independent experiments.
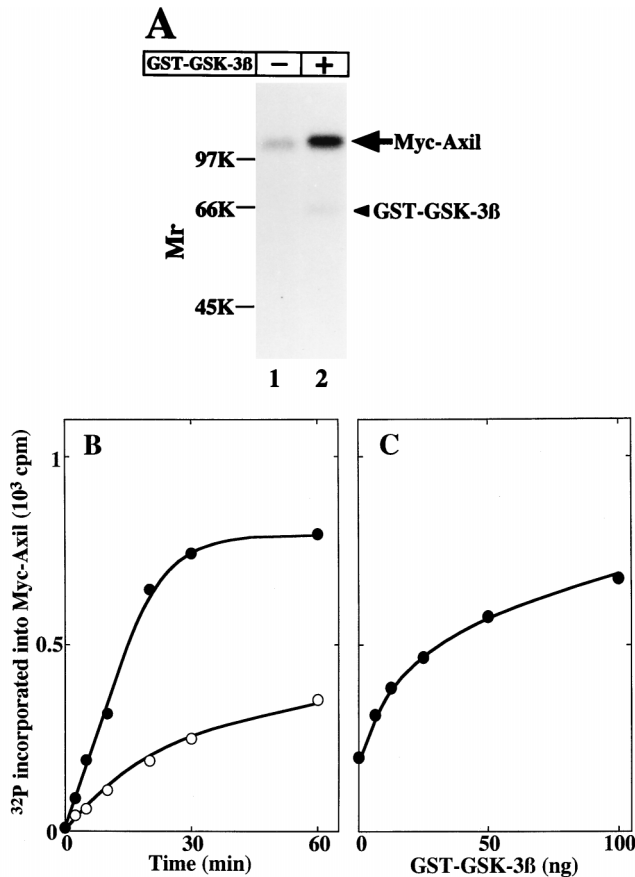
FIG. 4. Phosphorylation of Axil by GSK-3β. (A) Autoradiography. Myc-Axil immunoprecipitated from COS cell lysates (250 μg of protein) was incubated with (lane 2) or without (lane 1) GST–GSK-3β (100 ng of protein) for 20 min, and the samples were subjected to SDS-PAGE followed by autoradiography. The arrow and arrowhead indicate the positions of Myc-Axil and GST–GSK-3β, respectively. (B) Time course. Myc-Axil immunoprecipitated from COS cell lysates was incubated with (●) or without (○) GST–GSK-3β (100 ng of protein) for the indicated periods of time. (C) Dose dependency. Myc-Axil was incubated with the indicated amounts of GST–GSK-3β for 20 min. The results shown are representative of four independent experiments.

GSK-3β-dependent phosphorylation of β-catenin (Fig. 8C), it is unlikely that Axil activates GSK-3β kinase.

DISCUSSION

In a search for targets of GSK-3β-mediated determination of cell fate, we have identified Axil, an Axin homolog, as a GSK-3β-interacting protein. Axil displays the characteristics expected of a factor regulating axis formation in *Xenopus* embryos. Injection of Axil induces ventralization, and coinjection with Xwnt8 blocks Xwnt8-induced secondary axis formation. These results indicate that Axil has a function similar to that of Axin. The recent identification of Axin has provided an important insight into the Wnt-induced axis formation (45). Axin induces strong axis defects, a phenotype characteristic of completely ventralized embryos. Dorsal injection of Axin reduces the expression of the dorsal markers, Siamois, Goosecoid, and Chordin. Although Xwnt8, Xdsh, and kinase-negative GSK-3β induce a secondary axis, coinjection of Axin inhibits their activities. However, Axin did not affect secondary axis formation by β-catenin or Siamois. Thus, Axin regulates axis formation in *Xenopus* embryos by blocking the signaling through the Wnt pathway downstream of GSK-3β and upstream of β-catenin. Although the level at which Axil acts to inhibit the Wnt signaling pathway is not clear from our experiments using *Xenopus* embryos, the observations that Axil directly interacts with both GSK-3β and β-catenin and enhances GSK-3β-dependent phosphorylation of β-catenin suggest that Axil inhibits the Wnt signaling pathway by mediating the signal from GSK-3β to β-catenin. Taken together with the structural homology, it is possible that Axil and Axin have the same mode of action to regulate axis formation.

We have shown that Axil interacts with GSK-3β in COS cells and that the region containing residues 265 to 483 of Axil is responsible for the interaction. Axil interacts with the wild type but not a catalytically inactive mutant of GSK-3β. These results suggest that the interaction of GSK-3β with Axil requires the kinase activity of GSK-3β. We have demonstrated that Myc-Axil immunoprecipitated from COS cells and MBP-Axil(285-483) purified from *E. coli* are phosphorylated by GST–GSK-3β. The observations that Axil(265-483) binds to and is phosphorylated by GSK-3β directly indicate that the phos-
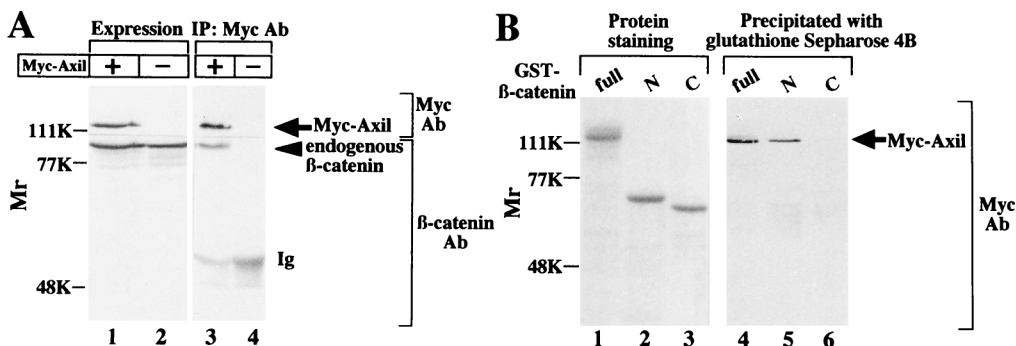

FIG. 5. Interaction of Axil with β-catenin in intact cells (A) and in vitro (B). (A) The lysates (20 μg of protein) of COS cells expressing Myc-Axil were probed with the anti-Myc and anti-β-catenin antibodies (lane 1). The same lysates (500 μg of protein) were immunoprecipitated with the anti-Myc antibody, and the immunoprecipitates were probed with the anti-Myc and anti-β-catenin antibodies (lane 3). The lysates of COS cells transfected with empty vectors were used as controls (lanes 2 and 4). (B) GST–β-catenin(full length) (lane 1), GST–N-terminal β-catenin (lane 2), and GST–C-terminal β-catenin (lane 3) (10 pmol each) were subjected to SDS-PAGE followed by Coomassie brilliant blue staining. After the lysates (500 μg of protein) of COS cells expressing Myc-Axil were incubated with GST–β-catenin (lane 4), GST–N-terminal β-catenin (lane 5), and GST–C-terminal β-catenin (lane 6) (50 pmol each), β-catenin and its deletion mutants were precipitated with glutathione Sepharose 4B. The precipitates were probed with the anti-Myc antibody. IP, immunoprecipitation; Ab, antibody; Ig, immunoglobulin; full, GST–β-catenin(full length); N, GST–N-terminal β-catenin; C, GST–C-terminal β-catenin. The arrows and arrowhead indicate the positions of Myc-Axil and endogenous β-catenin, respectively. The results shown are representative of three independent experiments.
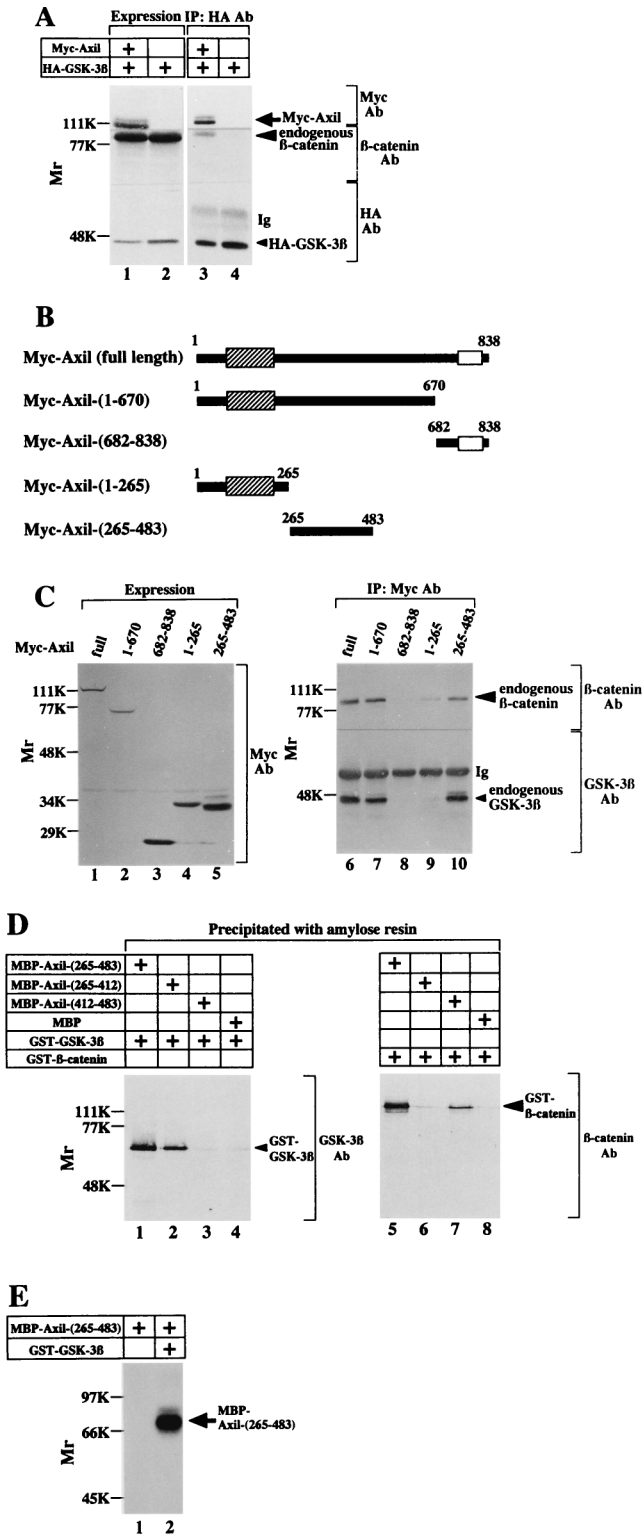
phorylation of Axil by GSK-3β requires their physical interaction.

Our results have shown that Axil interacts not only with GSK-3β but also with β-catenin and that the region containing residues 265 to 483 of Axil is also responsible for its binding to both proteins. In residues 265 to 483 of Axil, residues 265 to 412 and 412 to 483 are responsible for the binding to GSK-3β and β-catenin, respectively. Therefore, it is clear that GSK-3β and β-catenin bind to separate sites on Axil. Taken together with the observation that β-catenin is immunoprecipitated with GSK-3β in the presence of Axil, these results suggest that Axil, GSK-3β, and β-catenin make a ternary complex. However, to prove definitively this possibility, we have to demonstrate that all three components are present in a large complex in a gel filtration experiment. Furthermore, we have found that Axil promotes GSK-3β-dependent phosphorylation of β-catenin. The mechanism may involve the formation of a protein complex in which Axil brings together GSK-3β and β-catenin. Alternatively, Axil increases the affinity between GSK-3β and β-catenin. The stoichiometry of the phosphorylation of β-catenin by GSK-3β is still low even in the presence of Axil. Although we do not know the exact reason for this low stoichiometry, it might be due to the fact that Axil competes with β-catenin for the phosphorylation by GSK-3β since both proteins are substrates or that bacterially expressed proteins are used. It is well known that the phosphorylation of β-catenin is essential for its degradation (22). Therefore, Axil may cause the degradation of β-catenin by interacting with both GSK-3β and β-catenin and by enhancing the phosphorylation of β-catenin. This model is consistent with the observation that Axil negatively regulates the Wnt signaling pathway in development of *Xenopus* embryos. It has been shown that APC makes a complex with β-catenin and that the phosphorylation of APC by GSK-3β increases the binding of APC to β-catenin (37). Although it is not known whether APC promotes GSK-3β-dependent phosphorylation of β-catenin, APC and Axil may regulate the degradation of β-catenin by different mechanisms. At present, we do not know the physiological significance of the phosphorylation of Axil by GSK-3β for its functional interaction with GSK-3β and β-catenin.

Axil possesses the RGS homologous domain, as does Axin. Recently, a family of RGS proteins has been identified in eukaryotic species ranging from yeast to mammals (7). The RGS domain of this family member binds to the GTP-bound form of G_α and stimulates GTP hydrolysis of G_α. It has been shown that Wnt stimulates the phosphatidylinositol signaling pathway via G protein and that Wg-induced GSK-3 inactivation in-

FIG. 6. Complex formation of GSK-3β, Axil, and β-catenin. (A) Complex formation in intact cells. The lysates (20 μg of protein) of COS cells expressing HA–GSK-3β and Myc-Axil (lanes 1 and 3) and HA–GSK-3β alone (lanes 2 and 4) were probed with the anti-Myc, anti-β-catenin, and anti-HA antibodies (lanes 1 and 2). The same lysates (500 μg of protein) were immunoprecipitated with the anti-HA antibody, and the immunoprecipitates were probed with the anti-Myc, anti-β-catenin, and anti-HA antibodies (lanes 3 and 4). IP, immunoprecipitation, Ab, antibody; Ig, immunoglobulin. The arrow, large arrowhead, and small arrowhead indicate the positions of Myc-Axil, endogenous β-catenin, and HA–GSK-3β, respectively. (B) Deletion mutants of Axil. The hatched and empty boxes indicate the RGS and Dsh homologous domains, respectively. (C) Expression of Axil deletion mutants and their interaction with GSK-3β and β-catenin. The lysates (20 μg of protein) of COS cells expressing Myc-Axil(full length) (lane 1), Myc-Axil(1-670) (lane 2), Myc-Axil(682-838) (lane 3), Myc-Axil(1-265) (lane 4), and Myc-Axil(265-483) (lane 5) were probed with the anti-Myc antibody (left panel). The same lysates (500 to 1,000 μg of protein) (lanes 6 to 10) were immunoprecipitated with the anti-Myc antibody, and the immunoprecipitates were probed with the anti-GSK-3β and anti-β-catenin antibodies (right panel). The small and large arrowheads indicate the positions of endogenous GSK-3β and β-catenin, respectively. (D) Different binding sites of Axil for GSK-3β and β-catenin. After GST–GSK-3β (lanes 1 to 4) and GST–β-catenin (lanes 5 to 8) (8 pmol each) were incubated with MBP-Axil(265-483) (lanes 1 and 5), MBP-Axil(265-412) (lanes 2 and 6), MBP-Axil(412-483) (lanes 3 and 7), or MBP (lanes 4 and 8) (2 pmol each) immobilized on amylose resin, MBPs fused to proteins were precipitated by centrifugation. The precipitates were probed with the anti-GSK-3β and anti-β-catenin antibodies. The small and large arrowheads indicate the positions of GST–GSK-3β and GST–β-catenin, respectively. (E) Phosphorylation of Axil(265-483) by GSK-3β. MBP-Axil(265-483) (200 ng of protein) was incubated with (lane 2) or without (lane 1) GST–GSK-3β (100 ng of protein) for 30 min. The arrow indicates the position of MBP-Axil(265-483). The results shown are representative of three independent experiments.
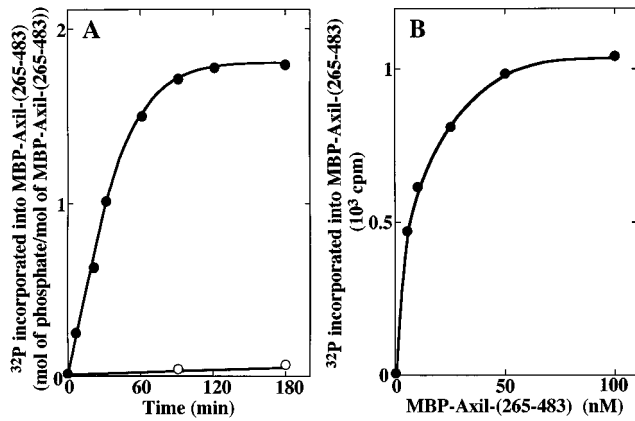
FIG. 7. Kinetics for the phosphorylation of Axil(265-483) by GSK-3β. (A) Time course. MBP-Axil(265-483) (200 ng of protein) purified from *E. coli* was incubated with (●) or without (○) GST–GSK-3β (100 ng of protein) for the indicated periods of time. (B) Dose dependency. The indicated concentrations of MBP-Axil(265-483) were incubated with GST–GSK-3β (100 ng of protein) for 20 min. The results shown are representative of three independent experiments.

volves protein kinase C (6, 39). Since the phosphatidylinositol turnover may be important in Wnt-induced degradation of β-catenin, it is intriguing to speculate that the RGS domain of Axil is a functional G_α GAP and thereby inhibits the Wnt signaling pathway. Alternatively, it may have an additional activity to transmit the signal by interacting with another protein(s). It has been shown that ΔRGS, a mutant of Axin in which the RGS domain is deleted, produces a secondary axis and that Axin blocks the axis-inducing activity of ΔRGS (45). These results indicate that ΔRGS acts through a dominant-negative mechanism to inhibit an endogenous Axin activity and that it competes for binding to a protein with which Axin normally interacts. Although we have not yet examined the effects of an RGS domain deletion mutant of Axil on axis formation of *Xenopus* embryos, our observation that the RGS domain of Axil is distinct from the GSK-3β- and β-catenin-binding sites suggests that the RGS domain deletion mutant of Axil also acts as a dominant negative form in the axis formation. Recently, we have found that the RGS domain of rAxin directly interacts with APC and that rAxin stimulates the degradation of β-catenin (17). Our result that Axil(1-265) containing the RGS domain makes a complex with β-catenin suggests that the RGS domain of Axil also interacts with APC which binds to β-catenin. Therefore, Axil and APC may also cooperatively regulate the stabilization of β-catenin. Besides the RGS domain, Axil has a domain homologous to the N-terminal region of Dsh. Since the function of this region of Dsh is not known, the
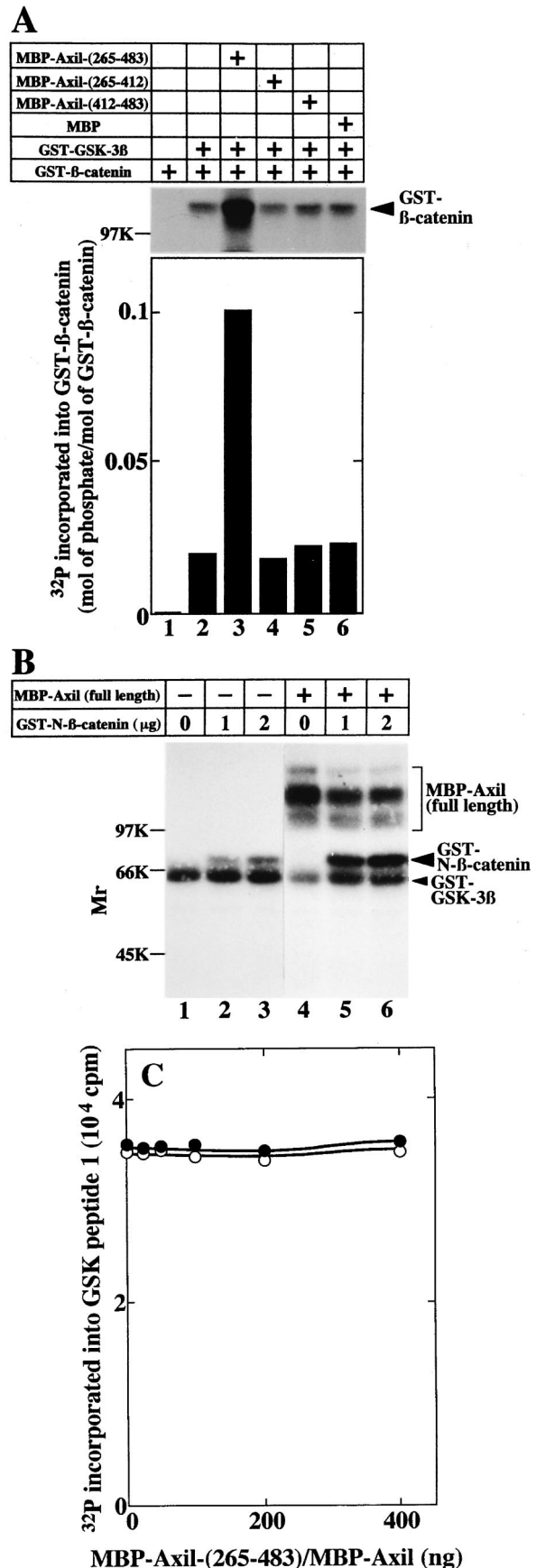

FIG. 8. Phosphorylation of β-catenin by GSK-3β in the presence of Axil. (A) Effect of MBP-Axil(265-483) on GSK-3β-dependent phosphorylation of β-catenin. GST–β-catenin (2 μg of protein) was incubated with GST–GSK-3β (600 ng of protein) in the presence of MBP-Axil(265-483) (lane 3), MBP-Axil(265-412) (lane 4), MBP-Axil(412-483) (lane 5), or MBP (lane 6) (200 ng of protein each) for 30 min. As a control, GST–β-catenin was incubated with (lane 2) or without (lane 1) GST–GSK-3β. (Upper panel) Autoradiography is shown. (Lower panel) The radioactivities incorporated into GST–β-catenin were counted and the stoichiometry of the phosphorylation was calculated. (B) Effect of full-length Axil on GSK-3β-dependent phosphorylation of β-catenin. The indicated amounts of GST–N-terminal β-catenin were incubated with GST–GSK-3β (400 ng of protein) in the presence (lanes 4 to 6) and absence (lanes 1 to 3) of MBP-Axil (160 ng of protein). GST–N-β-catenin, GST–N-terminal β-catenin. (C) Effect of Axil on GSK-3β activity. GST–GSK-3β (400 ng of protein) was incubated with 50 μM GSK peptide 1 in the presence of the indicated amounts of MBP-Axil(265-483) (●) or MBP-Axil (○). The results shown are representative of five independent experiments.

role of the Dsh homologous domain in the action of Axil remains to be clarified.

In addition to the regulation of development of *Xenopus lavies* and *Drosophila melanogaster*, β-catenin plays a role in promoting tumor formation in mammalian cells (32). A potential role for β-catenin in human cancer is supported by the findings that APC deletion mutants in colon cancer fail to downregulate levels of free β-catenin (26, 27). Furthermore, it has been shown that there are mutations of serine in the possible phosphorylation site of β-catenin for GSK-3β in melanoma and colon cancer that have normal APC protein (18, 25, 38). Thus, there are at least two ways by which levels of free β-catenin increase due to mutations in APC and β-catenin itself. Therefore, mutations in GSK-3β- and β-catenin-binding sites on Axil may cause human cancer. Further investigations are necessary to fully elucidate the functions of the Axin family in cellular proliferation and differentiation.

REFERENCES

1. **Aberle, H., A. Bauer, J. Stappert, A. Kispert, and R. Kemler.** 1997. β-Catenin is a target for the ubiquitin-proteasome pathway. EMBO J. **16:**3797–3804.
2. **Behrens, J., J. P. von Kries, M. Kühl, L. Bruhn, D. Wedlich, R. Grosschedl, and W. Birchmeier.** 1996. Functional interaction of β-catenin with the transcription factor LEF-1. Nature **382:**638–642.
3. **Bhanot, P., M. Brink, C. H. Samos, J. C. Hsieh, Y. Wang, J. P. Macke, D. Andrew, J. Nathans, and R. Nusse.** 1996. A new member of the *frizzled* family from *Drosophila* functions as a Wingless receptor. Nature **382:**225–230.
4. **Bradford, M. M.** 1976. A rapid and sensitive method for the quantitation of microgram quantities of protein utilizing the principle of protein-dye binding. Anal. Biochem. **72:**248–254.
5. **Cadigan, K. M., and R. Nusse.** 1997. Wnt Meeting 1996. Biochim. Biophys. Acta **1332:**R1–R5.
6. **Cook, D., M. J. Fry, K. Hughes, R. Sumathipala, J. R. Woodgett, and T. C. Dale.** 1996. Wingless inactivates glycogen synthase kinase-3 via an intracellular signalling pathway which involves a protein kinase C. EMBO J. **15:**4526–536.
7. **Dohlman, H. G., and J. Thorner.** 1997. RGS proteins and signaling by heterotrimeric G proteins. J. Biol. Chem. **272:**3871–3874.
8. **Druey, K. M., K. J. Blumer, V. H. Kang, and J. H. Kehrl.** 1996. Inhibition of G-protein-mediated MAP kinase activation by a new mammalian gene family. Nature **379:**742–746.
9. **Glueecksohn-Schoenheimer, S.** 1949. The effects of a lethal mutation responsible for duplications and twinning in mouse embryos. J. Exp. Zool. **110:**47–76.
10. **He, X., J. P. Saint-Jeannet, J. R. Woodgett, H. E. Varmus, and I. B. Dawid.** 1995. Glycogen synthase kinase-3 and dorsoventral patterning in *Xenopus* embryos. Nature **374:**617–622.
11. **Hinoi, T., S. Kishida, S. Koyama, M. Ikeda, Y. Matsuura, and A. Kikuchi.** 1996. Post-translational modifications of Ras and Ral are important for the action of Ral GDP dissociation stimulator. J. Biol. Chem. **271:**19710–19716.
12. **Ikeda, M., O. Ishida, T. Hinoi, S. Kishida, and A. Kikuchi.** 1998. Identification and characterization of a novel protein interacting with Ral-binding protein 1, a putative effector protein of Ral. J. Biol. Chem. **273:**814–821.
13. **Ikeda, S., S. Kishida, H. Yamamoto, H. Murai, S. Koyama, and A. Kikuchi.** 1998. Axin, a negative regulator of the Wnt signaling pathway, forms a complex with GSK-3β and β-catenin and promotes GSK-3β-dependent β-catenin phosphorylation. EMBO J. **17:**1371–1384.
14. **Jacobs-Cohen, R. J., M. Spiegelman, J. C. Cookingham, and D. Bennett.** 1984. Knobbly, a new dominant mutation in the mouse that affects embryonic ectoderm organization. Genet. Res. **43:**43–50.
15. **Kao, K. R., and R. P. Elinson.** 1988. The entire mesodermal mantle behaves as Spemann's organizer in dorsoanterior enhanced *Xenopus lavies* embryos. Dev. Biol. **127:**64–77.
16. **Kikuchi, A., and L. T. Williams.** 1996. Regulation of interaction of *ras* p21 with RalGDS and Raf-1 by cyclic AMP-dependent protein kinase. J. Biol. Chem. **271:**588–594.
17. **Kishida, S., H. Yamamoto, S. Ikeda, M. Kishida, I. Sakamoto, S. Koyama, and A. Kikuchi.** Axin, a negative regulator of the Wnt signaling pathway, directly interacts with APC and regulates the stabilization of β-catenin. J. Biol. Chem., in press.
18. **Korinek, V., N. Barker, P. J. Morin, D. van Wichen, R. de Weger, K. W. Kinzler, B. Vogelstein, and H. Clevers.** 1997. Constitutive transcriptional activation by a β-catenin-Tcf complex in APC$^{-/-}$ colon carcinoma. Science **275:**1784–1787.
19. **Kozak, M.** 1987. An analysis of 5'-noncoding sequences from 699 vertebrate messenger RNAs. Nucleic Acids Res. **15:**8125–8148.
20. **Kreig, P. A., and D. A. Melton.** 1984. Functional messenger RNAs are produced by SP6 *in vitro* transcription of cloned cDNAs. Nucleic Acids Res. **12:**7057–7070.
21. **Maniatis, T.** 1982. Molecular cloning: a laboratory manual. Cold Spring Harbor Laboratory, Cold Spring Harbor, N.Y.
22. **Miller, J. R., and R. T. Moon.** 1996. Signal transduction through β-catenin and specification of cell fate during embryogenesis. Genes Dev. **10:**2527–2539.
23. **Mizushima, S., and S. Nagata.** 1990. pEF-BOS, a powerful mammalian expression vector. Nucleic Acids Res. **18:**5322.
24. **Molenaar, M., M. van de Wetering, M. Oosterwegel, J. Peterson-Maduro, S. Godsave, V. Korinek, J. Roose, O. Destrée, and H. Clevers.** 1996. XTcf-3 transcription factor mediates β-catenin-induced axis formation in *Xenopus* embryos. Cell **86:**391–399.
25. **Morin, P. J., A. B. Sparks, V. Korinek, N. Barker, H. Clevers, B. Vogelstein, and K. W. Kinzler.** 1997. Activation of β-catenin-Tcf signaling in colon cancer by mutations in β-catenin or APC. Science **275:**1787–1790.
26. **Munemitsu, S., I. Albert, B. Rubinfeld, and P. Polakis.** 1996. Deletion of an amino-terminal sequence stabilizes β-catenin in vivo and promotes hyperphosporylation of the adenomatous polyposis coli tumor suppressor protein. Mol. Cell. Biol. **16:**4088–4094.
27. **Munemitsu, S., I. Albert, B. Souza, B. Rubinfeld, and P. Polakis.** 1995. Regulation of intracellular β-catenin levels by the adenomatous polyposis coli (APC) tumor-suppressor protein. Proc. Natl. Acad. Sci. USA **92:**3046–3050.
28. **Murai, H., M. Ikeda, S. Kishida, O. Ishida, M. Okazaki-Kishida, Y. Matsuura, and A. Kikuchi.** 1997. Characterization of Ral GDP dissociation stimulator-like (RGL) activities to regulate *c-fos* promoter and the GDP/GTP exchange of Ral. J. Biol. Chem. **272:**10483–10490.
29. **Murai, H., M. Okazaki, and A. Kikuchi.** 1996. Tyrosine dephosphorylation of glycogen synthase kinase-3 is involved in its extracellular signal-dependent inactivation. FEBS Lett. **392:**153–160.
30. **Nusse, R.** 1997. A versatile transcriptional effector of Wingless signaling. Cell **89:**321–323.
31. **Nusse, R., and H. E. Varmus.** 1992. Wnt genes. Cell **69:**1073–1087.
32. **Peifer, M.** 1997. β-Catenin as oncogene: the smoking gun. Science **275:**1752–1753.
33. **Perry, W. L., III, T. J. Vasicek, J. J. Lee, J. M. Rossi, L. Zeng, T. Zhang, S. M. Tilghman, and F. Costantini.** 1995. Phenotypic and molecular analysis of a transgenic insertional allele of the mouse *Fused* locus. Genetics **141:**321–332.
34. **Plyte, S. E., K. Hughes, E. Nikolakaki, B. J. Pulverer, and J. R. Woodgett.** 1992. Glycogen synthase kinase-3: functions in oncogenesis and development. Biochim. Biophys. Acta **1114:**147–162.
35. **Polakis, P.** 1997. The adenomatous polyposis coli (APC) tumor suppressor. Biochim. Biophys. Acta **1332:**F127–F147.
36. **Reed, S. C.** 1937. The inheritance and expression of Fused, a new mutation in the house mouse. Genetics **22:**1–13.
37. **Rubinfeld, B., I. Albert, E. Porfiri, C. Fiol, S. Munemitsu, and P. Polakis.** 1996. Binding of GSK3β to the APC-β-catenin complex and regulation of complex assembly. Science **272:**1023–1026.
38. **Rubinfeld, B., P. Robbins, M. El-Gamil, I. Albert, E. Porfiri, and P. Polakis.** 1997. Stabilization of β-catenin by genetic defects in melanoma cell lines. Science **275:**1790–1792.
39. **Slusarski, D. C., V. G. Corces, and R. T. Moon.** 1997. Interaction of Wnt and a Frizzled homologue triggers G-protein-linked phosphatidylinositol signaling. Nature **390:**410–413.
40. **Sokol, S., J. L. Christian, R. T. Moon, and D. A. Melton.** 1991. Injected Wnt RNA induces a complete body axis in *Xenopus* embryos. Cell **67:**741–752.
41. **Sussman, D. J., J. Klingensmith, P. Salinas, P. S. Adams, R. Nusse, and N. Perrimon.** 1994. Isolation and characterization of a mouse homolog of the *Drosophila* segment polarity gene *dishevelled*. Dev. Biol. **166:**73–86.
42. **Vojtek, A. B., S. M. Hollenberg, and J. A. Cooper.** 1993. Mammalian Ras interacts directly with the serine/threonine kinase Raf. Cell **74:**205–214.
43. **Wang, Q. M., C. J. Fiol, A. A. DePaoli-Roach, and P. J. Roach.** 1994. Glycogen synthase kinase-3β is a dual specificity kinase differentially regulated by tyrosine and serine/threonine phosphorylation. J. Biol. Chem. **269:**14566–14574.
44. **Yost, C., M. Torres, J. R. Miller, E. Huang, D. Kimelman, and R. T. Moon.** 1996. The axis-inducing activity, stability, and subcellular distribution of β-catenin is regulated in *Xenopus* embryos by glycogen synthase kinase 3. Genes Dev. **10:**1443–1454.
45. **Zeng, L., F. Fagotto, T. Zhang, W. Hsu, T. J. Vasicek, W. L. Perry III, J. J. Lee, S. M. Tilghman, B. M. Gumbiner, and F. Costantini.** 1997. The mouse *Fused* locus encodes Axin, an inhibitor of the Wnt signaling pathway that regulates embryonic axis formation. Cell **90:**181–192.